

## Article

# High Wet Deposition of Black Carbon over the Sichuan Basin of China

Yu Zhou <sup>1,2</sup>, Xiaolin Zhang <sup>1,2,3,\*</sup>  and Yuanzhi Wang <sup>1,2</sup>

<sup>1</sup> Key Laboratory of Meteorological Disaster, Ministry of Education (KLME), Nanjing University of Information Science & Technology, Nanjing 210044, China

<sup>2</sup> Key Laboratory for Aerosol-Cloud-Precipitation of China Meteorological Administration, School of Atmospheric Physics, Nanjing University of Information Science & Technology, Nanjing 210044, China

<sup>3</sup> Department of Earth and Environmental Sciences, The University of Manchester, Manchester M13 9PL, UK

\* Correspondence: xlnzhang@nuist.edu.cn

**Abstract:** The wet deposition flux of black carbon (BC) over the Sichuan Basin is studied on the basis of the MERRA-2 data from 1981 to 2020, aiming at investigating high BC wet deposition flux in China in terms of long-term spatial-temporal trends and influences of BC column mass density and precipitation. In China, the largest BC wet deposition flux with a regionally-averaged value of  $1.00 \times 10^{-2} \mu\text{g m}^{-2} \text{s}^{-1}$  over the Sichuan Basin is observed, especially in the western and southern regions of the Basin with values as high as  $2.20 \times 10^{-2} \mu\text{g m}^{-2} \text{s}^{-1}$ . The seasonality of BC wet deposition flux over the Sichuan Basin depicts maximum levels in autumn, moderate levels in spring and winter, and minimum levels in summer. The monthly mean BC wet deposition flux varies almost twofold, ranging from the lowest average value of  $8.05 \times 10^{-3} \mu\text{g m}^{-2} \text{s}^{-1}$  in July to the highest  $1.28 \times 10^{-2} \mu\text{g m}^{-2} \text{s}^{-1}$  in October. This study suggests that BC column mass density and precipitation are two significant factors affecting high BC wet deposition flux, whereas BC wet deposition flux is more related to BC column mass density than to precipitation over the Sichuan Basin.

**Keywords:** black carbon; wet deposition; MERRA-2; Sichuan Basin



**Citation:** Zhou, Y.; Zhang, X.; Wang, Y. High Wet Deposition of Black Carbon over the Sichuan Basin of China. *Atmosphere* **2023**, *14*, 598. <https://doi.org/10.3390/atmos14030598>

Academic Editors: Panu Karjalainen and Kumar Vikrant

Received: 22 January 2023

Revised: 11 March 2023

Accepted: 17 March 2023

Published: 21 March 2023



**Copyright:** © 2023 by the authors. Licensee MDPI, Basel, Switzerland. This article is an open access article distributed under the terms and conditions of the Creative Commons Attribution (CC BY) license (<https://creativecommons.org/licenses/by/4.0/>).

## 1. Introduction

Black carbon (BC) aerosols are mainly generated from the incomplete combustion of biomass and fossil fuels [1,2] and are one of the important components of atmospheric particulate matter with unique physicochemical properties [3]. BC is considered the second strongest warming factor (behind only carbon dioxide) on climate change in the present atmosphere [1]; thus, it has attracted a good deal of attention because of its important local and global climate impacts. Dry and wet depositions are the main pathways for the removal of BC particles from the atmosphere [4–7] and are the key processes in which regional emitted BC enter the surface ecosystem [8]. Dry deposition includes gravitational sedimentation and direct capture through contact with vegetation and other surface objects, while wet deposition is associated with rainfall or snowfall in which the particles serve as cloud condensation nuclei and there is a subsequent flush of particles during precipitation [9]. Wet deposition is even more significant than dry deposition in maintaining a balance between aerosol emissions and deposition [10–13]. The efficiency of removing aerosols by wet deposition depends on particle size [14]; wet deposition is most effective for a particle diameter larger than  $2 \mu\text{m}$ , because aerosols are most easily captured by droplets due to a high collision efficiency coefficient [15,16].

Previous studies have examined atmospheric nitrogen and sulfur deposition, showing spatial variability in nitrogen or sulfur deposition as a result of natural and anthropogenic factors [17–19]. Meanwhile, multiple studies have reported the spatial and seasonal variations in the wet deposition of carbonaceous aerosols including organic carbon (OC) and

elemental carbon (EC) [8,20,21]. At present, most studies are conducted to calculate the wet deposition flux through the EC and OC concentrations in precipitation measured by different measurement methods [22–26]. The global wet deposition of dissolved organic carbon accounts for 430 Tg C/year [27], while the wet deposition of black carbon is about 80% of the global BC deposition [20,28]. Wet deposition is the main way to remove atmospheric particulates [6], and precipitation affects the wet deposition of black carbon [29]. Wet deposition has different characteristics in urban and rural areas [8,18]. For example, the high value of dissolved OC wet deposition is observed in rural areas of the Amazon [30]. The analysis of backward trajectory shows that the long-distance transportation of air mass is also an important factor affecting wet deposition [31,32]. Zhao et al. present the short-term time change in wet deposition of EC and water-insoluble organic carbon measured by the thermo-optic method in Xiamen [33]. Wet deposition in northern China shows similar seasonal changes [34], and this may be due to seasonal variations in human activities or weather conditions such as temperature and precipitation [35]. Because of the extensive emission of BC, the study of BC deposition is particularly important in areas with frequent human activities [36]. Although significant studies regarding short-term BC wet deposition have been performed [29,37,38], there have been few studies reporting long-term spatial-temporal patterns of wet deposition in China.

Here, long-term characteristics of BC wet deposition flux in the Sichuan Basin based on the MERRA-2 data during 1981–2020 are studied. The aim of this paper is to evaluate the spatial distribution of BC wet deposition in China and to assess the long-term spatial-temporal patterns regarding annual, seasonal, and monthly variations in high BC wet deposition in the Sichuan Basin, as well as impacts by BC column mass density and precipitation. The results can help us better understand black carbon removal in the atmosphere so as to provide a scientific basis for the atmospheric environment and ecological balance.

## 2. Methodology

### 2.1. Targeted Area

The geographical location of the selected research area is shown in Figure 1. Located in southwestern China, the Sichuan Basin (28° N–32° N, 103° E–108° E) covers about 260,000 km<sup>2</sup>. The Sichuan Basin has one of the severest cases of air pollution in China, with dense population and industry distribution due to strong anthropogenic emissions and special terrains [39]. Moreover, the Sichuan Basin has the highest topographic relief across the basin [40].

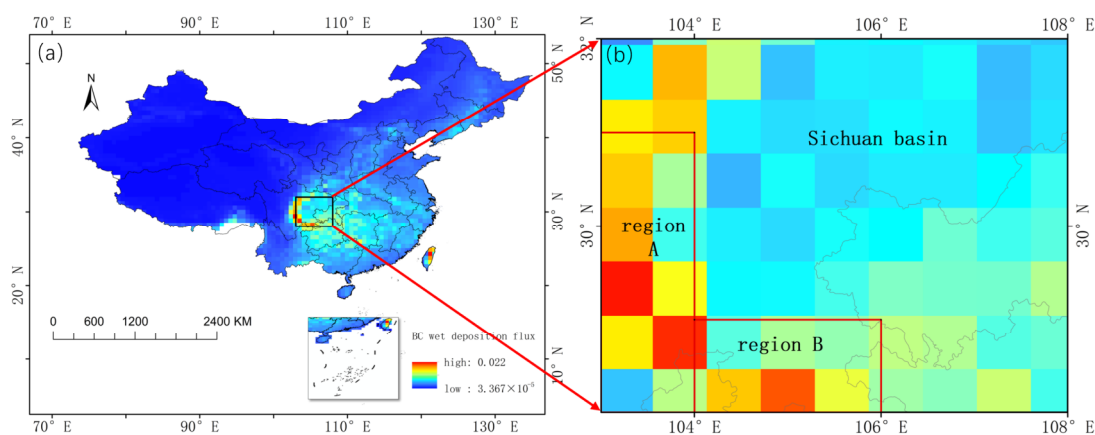


**Figure 1.** Location of the site selected in this study (a). Black box denotes the study area of the Sichuan basin (28° N–32° N, 103° E–108° E) in China (b). Red boxes denote the study areas with high BC wet deposition values over the western (region A) and southern (region B) parts of Sichuan Basin. Unit:  $\mu\text{g m}^{-2} \text{s}^{-1}$ .

## 2.2. MERRA-2 Dataset

We used version 2 of the Modern-Era Retrospective Analysis for Research and Applications (MERRA-2) reanalysis dataset produced by the Goddard Earth Observing System Model, Version 5 (GEOS-5) [41]. The MERRA-2 includes for the first time analyzed aerosol fields that are radiatively coupled to the atmosphere, and aerosol and meteorological observations are jointly assimilated in the MEERA-2 with the aim of producing integrated Earth system analysis [42,43]. The MERRA-2 provides a spatial resolution of  $0.5^\circ \times 0.625^\circ$  and 72 vertical model levels from 1000 hPa to 0.1 hPa; in addition, there are 1-hourly, 3-hourly, and monthly MERRA-2 products [44]. The MERRA-2 is the most significant long-term global reanalysis and represents their interaction with other physical processes in the climate system [45]. The monthly MERRA-2 datasets for BC wet deposition flux, as well as BC column mass density and precipitation, are employed in this study.

## 2.3. Pearson Correlation Coefficient

The study shows that BC column mass density and precipitation are the two most important influencing factors in response to BC wet deposition flux [29,34]. Therefore, this study considers BC column mass density and precipitation as the main influential factors affecting the space-time change in BC wet deposition flux for conducting correlation analysis. The correlation coefficient  $R_{xy}$  is calculated as follows:

$$R_{xy} = \frac{\sum_{i=1}^n [(x_i - \bar{x})(y_i - \bar{y})]}{\sqrt{\sum_{i=1}^n (x_i - \bar{x})^2} \cdot \sqrt{\sum_{i=1}^n (y_i - \bar{y})^2}},$$

where  $R_{xy}$  is the correlation coefficient of variables  $x$  and  $y$ ;  $X_i$  is BC wet deposition flux in the  $i$ th year;  $Y_i$  is the value of the impact factor in the  $i$ th year; BC column mass density (unit:  $\text{mg m}^{-2}$ ) and precipitation (unit:  $\mu\text{g m}^{-2} \text{s}^{-1}$ ) are the impact factors; and  $\bar{x}$  and  $\bar{y}$  are the mean values of BC wet deposition flux and influence factors during  $n$  years, respectively.

## 3. Results and Discussion

### 3.1. Annual Trends of BC Wet Deposition

As shown in Figure 1, significantly larger BC wet deposition fluxes are observed over the Sichuan Basin than in other areas of China, with a particular concentration in the western and southern regions of the Sichuan Basin. The characteristics of BC wet deposition fluxes in the Sichuan Basin are systematically investigated in the following. Figure 2 shows the spatial distributions of decade mean BC wet deposition flux in the Sichuan Basin from 1981 to 2020. The distributions of BC wet deposition flux depict high values exceeding  $1.20 \times 10^{-2} \mu\text{g m}^{-2} \text{s}^{-1}$  in the western and southern regions of the Sichuan Basin. For decade variation, the distributions of BC wet deposition flux show similar patterns, and the areas with high BC wet deposition flux become slightly smaller during the recent decade of 2011–2020. The BC wet deposition flux is probably related to BC emissions and the amount of precipitation [46]. The BC wet deposition flux obtained in the Sichuan Basin is higher than that over the Changbai Mountains, which are in a range of  $0.09\text{--}1.44 \mu\text{g cm}^{-2} \text{month}^{-1}$  [24].

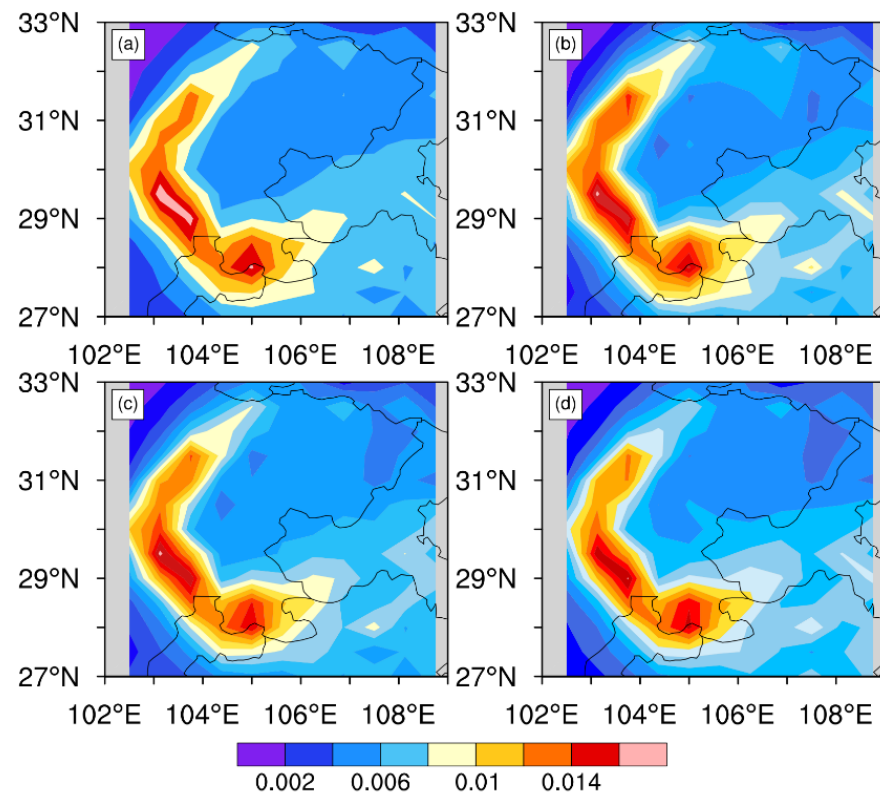


**Figure 2.** Spatial distribution of decade mean black carbon wet deposition flux over the study area in the Sichuan Basin during 1981–1990 (a), 1991–2000 (b), 2001–2010 (c), and 2011–2020 (d). Unit:  $\mu\text{g m}^{-2} \text{s}^{-1}$ .

The annual variations in BC wet deposition flux in the Sichuan Basin from 1981 to 2020 are shown in Figure 3. In the past 40 years, mean BC wet deposition flux in the Sichuan Basin is found to be  $1.00 \times 10^{-2} \mu\text{g m}^{-2} \text{s}^{-1}$ . The annual-averaged BC wet deposition flux in the Sichuan Basin is higher than that in the urban city of Tokyo [47], in the rural city of Averiro, and in a mountain region in Germany [10]. The high wet deposition flux in the Sichuan Basin may have a negative impact on the environmental ecosystem in the Basin. As shown in Figure 3a, the highest value of BC wet deposition flux is  $1.44 \times 10^{-2} \mu\text{g m}^{-2} \text{s}^{-1}$  in 2004, and the lowest is  $6.53 \times 10^{-3} \mu\text{g m}^{-2} \text{s}^{-1}$  in 1982. The annual trend of BC wet deposition flux is generally similar to the trends of  $\text{NO}_3^-$  in Zhang et al. [48] and Cao et al. [49]. This is probably due to the annual trends of BC concentration. As shown in Figure 3b, the BC wet deposition flux during 2001–2010 is the highest among the four decades with a mean value of  $1.29 \times 10^{-2} \mu\text{g m}^{-2} \text{s}^{-1}$ . Low BC wet deposition fluxes are seen during the periods of 1981–1990 and 1991–2000, with the average values being  $7.80 \times 10^{-3}$  and  $8.31 \times 10^{-3} \mu\text{g m}^{-2} \text{s}^{-1}$ , respectively. Since 2000, industry and energy have developed rapidly in China, and various particulate matters including black carbon have increased. To reduce the generation of particulate matter, the Chinese government is taking action regarding the reduction in greenhouse gas emission during the “12th Five-Year Plan” (2011–2015) and the intensity of carbon emissions during the “13th Five-Year Plan” (2016–2020) periods [50]. This may be one of the reasons for the decrease in BC wet deposition flux from 2011 to 2020.

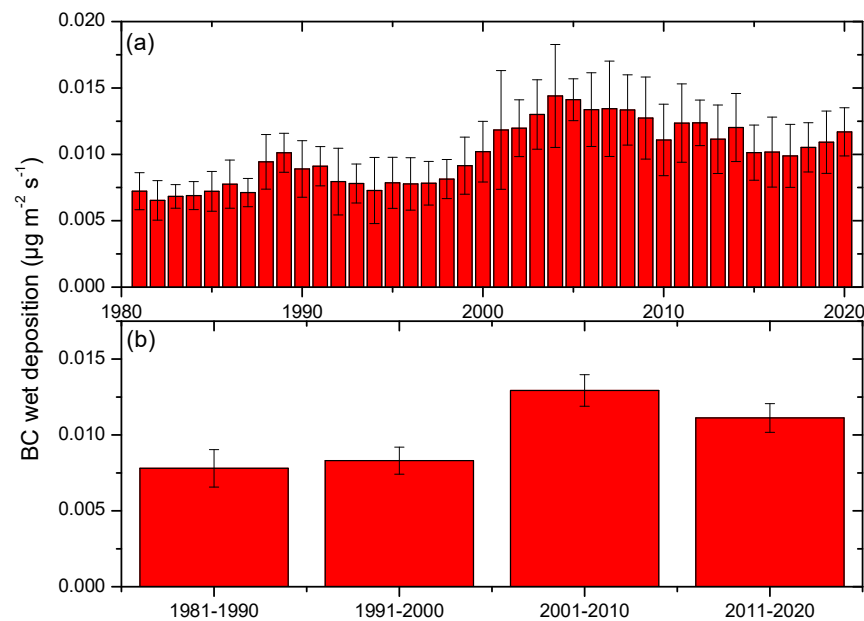


**Figure 3.** Annual variations of area-averaged black carbon wet deposition flux over the Sichuan basin from 1981 to 2020 (a) and in four periods (b) during 1981–1990, 1991–2000, 2001–2010 and 2011–2020.

### 3.2. Seasonal and Monthly Patterns of BC Wet Deposition

The spatial distribution of BC wet deposition flux over the Sichuan Basin from 1981 to 2020 shows obvious seasonality, which is illustrated in Figure 4. BC wet deposition fluxes are generally much higher in the western regions than in the eastern regions of the Sichuan Basin in all seasons. High BC wet deposition fluxes in the southwestern regions of the Sichuan Basin are seen in spring, autumn, and winter, as opposed to high values in the northwestern regions in summer. Moreover, significantly evident spatial differences in BC wet deposition flux are seen between the western and eastern parts of the Sichuan Basin in summer (see Figure 4b). The strongest BC wet deposition fluxes are observed in the southwestern part of the Sichuan Basin in autumn, with values exceeding  $2.0 \times 10^{-2} \mu\text{g m}^{-2} \text{s}^{-1}$  (see Figure 4c). The Sichuan Basin shows a higher altitude in the northwest and a lower altitude in the southeast, and the north wind prevailing in winter can transport the pollutants from north to south; this probably results in higher BC wet deposition flux in the southern region attributed to the accumulation of BC pollutants caused by the long-distance transportation of air masses [51–53].

The seasonal distribution of mean BC wet deposition flux during the past 40 years is shown in Figure 5. As shown in Figure 5a, the autumn season shows the highest wet deposition flux, with an average value of  $1.18 \times 10^{-2} \mu\text{g m}^{-2} \text{s}^{-1}$ , followed by spring and winter with values of  $1.02 \times 10^{-2}$  and  $9.31 \times 10^{-3} \mu\text{g m}^{-2} \text{s}^{-1}$ , respectively, while summer has relatively lower wet deposition flux with a mean value of  $8.81 \times 10^{-3} \mu\text{g m}^{-2} \text{s}^{-1}$ . The BC wet deposition fluxes during four decades show similar seasonality (see Figure 5b). The wet deposition of black carbon during 1981–2000 is lower than the average BC wet deposition in the past 40 years, and the BC wet deposition flux in each season is high during 2001–2020. High BC wet deposition fluxes in autumn are seen in all four decades. The high wet deposition flux occurring in fall possibly corresponds to the high level of BC concentration during this period over the Sichuan Basin [54]. In summer, the BC wet deposition flux is low while the precipitation and BC concentration are large [33]. It is documented that the sparse precipitation amount may induce low BC wet deposition flux in winter [55]. The BC wet deposition flux in the Sichuan Basin obtained in our study is significantly larger than that seen in Lhasa [20] but lower than that seen in Shanghai [8]. Compared with human activities in the Sichuan Basin and Shanghai, there are fewer human activities in Lhasa, indicating that human activities may have an impact on BC wet deposition flux.

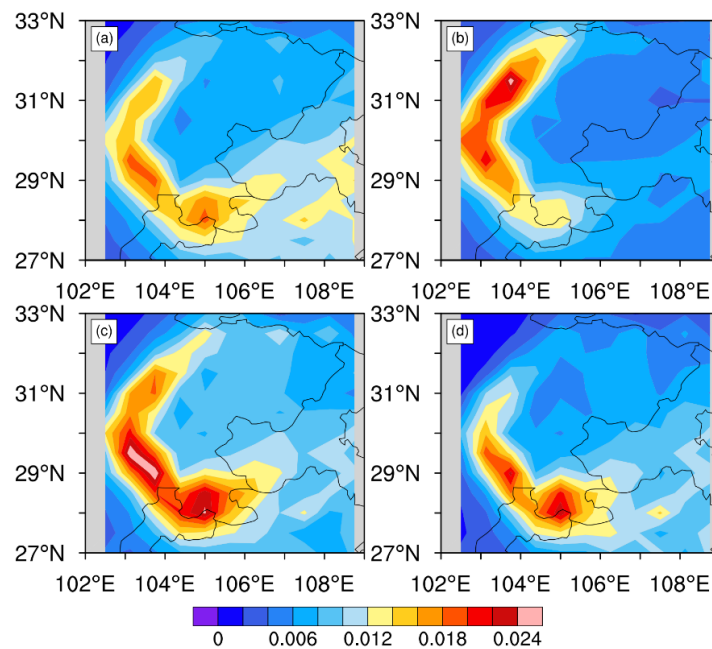


**Figure 4.** Mean spatial distribution of black carbon wet deposition flux in spring (a), summer (b), autumn (c), and winter (d) over the Sichuan Basin during 1981–2020. Unit:  $\mu\text{g m}^{-2} \text{s}^{-1}$ .

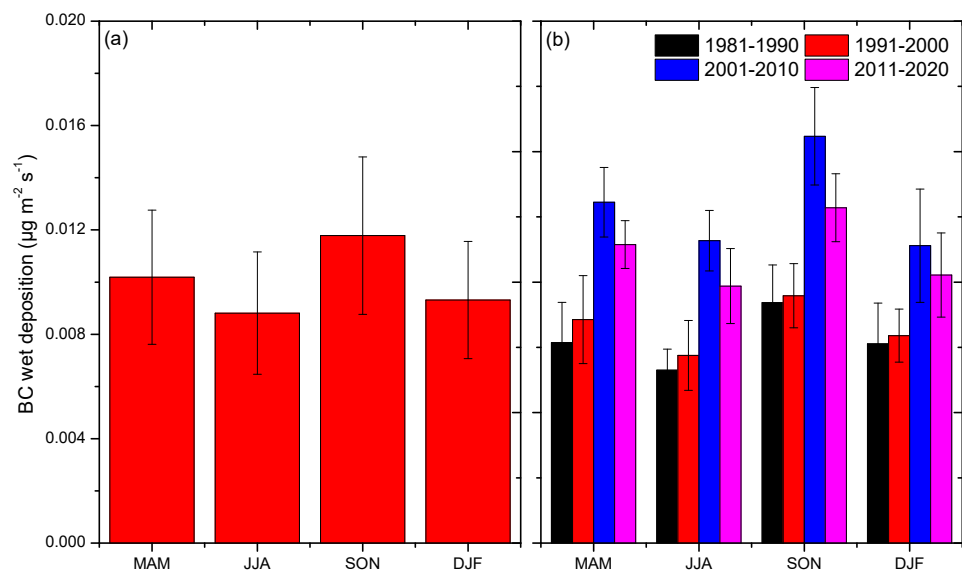


**Figure 5.** Seasonal variations of area-averaged black carbon wet deposition flux over the Sichuan Basin from 1981 to 2020 (MAM, JJA, SON and DJF represent spring, summer, autumn, and winter, respectively) (a) and in four periods (b) during 1981–1990, 1991–2000, 2001–2010, and 2011–2020.

The spatial distribution of monthly average BC wet deposition flux over the Sichuan Basin from 1981 to 2020 is illustrated in Figure 6. The monthly patterns of spatial distributions of BC wet deposition fluxes are generally in accordance with their seasonal patterns. High BC wet deposition fluxes in the northwestern parts of the Sichuan Basin are seen in July and August, whereas high values in the southwestern regions are observed in other months. Monthly BC wet deposition flux shows large variability, being mainly due to the variability in BC concentration and precipitation [20,46]. The monthly mean BC wet deposition fluxes over the Sichuan Basin from 1981 to 2020 are shown in Figure 7. Monthly mean BC wet deposition fluxes vary almost twofold, from the lowest average value of  $8.05 \times 10^{-3} \mu\text{g m}^{-2} \text{s}^{-1}$  in July to the highest  $1.28 \times 10^{-2} \mu\text{g m}^{-2} \text{s}^{-1}$  in October (see Figure 7a). Zhou et al. observes that the wet deposition flux of organic carbon is

low in May and high in July in Changsha [56], which differs from the trends of BC wet deposition flux in our study. There is a significant correlation between wet deposition and precipitation in Changsha; the annual maximum precipitation of Changsha in July is more than 300 mm [56], which may be one of the reasons for the high wet deposition flux of Changsha in July. Organic carbon concentration of Changsha in May is relatively lower than those in other months [56], and therefore, the low value of wet deposition in Changsha may have some relation to organic carbon concentrations. The monthly variations in BC wet deposition flux in the four decades from 1981 to 2020 are shown in Figure 7b. The monthly-averaged BC wet deposition fluxes in the Sichuan Basin from 1981 to 1990 and from 1991 to 2000 are much smaller than those during 2001–2010 and 2011–2020. The BC wet deposition flux from 1981 to 1990 is slightly lower than that during 1991–2000. The BC wet deposition fluxes during the four decades generally show similar monthly variations, with high values in October and low values in July. The high temperature in July aggravates the weather disturbance and vertical mixing, resulting in a decrease in BC concentration; this may be part of the reason for the low BC wet deposition flux [57]. Biomass combustion occurs frequently in autumn, especially October [58], exacerbating the accumulation of BC concentration and leading to the high BC wet deposition flux in October.

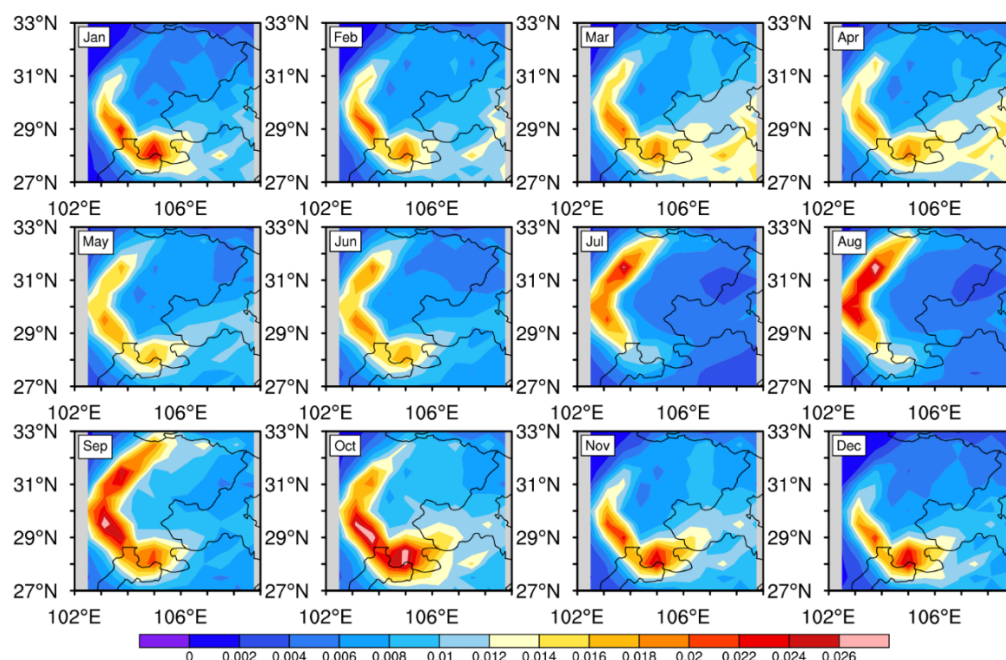


**Figure 6.** Spatial distribution of monthly variations of black carbon wet deposition flux over the Sichuan Basin during 1981–2020. Unit:  $\mu\text{g m}^{-2} \text{s}^{-1}$ .

### 3.3. Factors Influencing BC Wet Deposition

To a great extent, the wet deposition flux of black carbon is believed to be controlled by precipitation and BC loading in the atmosphere [46,55,59]. The relationships between BC wet deposition flux and BC column mass density and precipitation are illustrated in Figure 8. As shown in Figure 8a, a weak positive correlation is found between BC wet deposition flux and BC column mass density, indicating that more BC particles are a benefit for larger BC wet deposition flux. Positive correlations between concentrations of atmospheric compositions and their wet deposition flux are also found in Zhang et al. [60] and Yu et al. [61]. The relationship between BC wet deposition flux and precipitation is shown in Figure 8b, and a poor positive correlation is seen. Larger precipitation density can scavenge more BC aerosols and leads to a higher BC wet deposition flux. Similar impacts of precipitation on the wet depositions of aerosols and atmospheric compositions are presented in many previous studies [62–64]. Therefore, compared with precipitation, the distribution of BC wet deposition flux is more affected by BC column mass density.

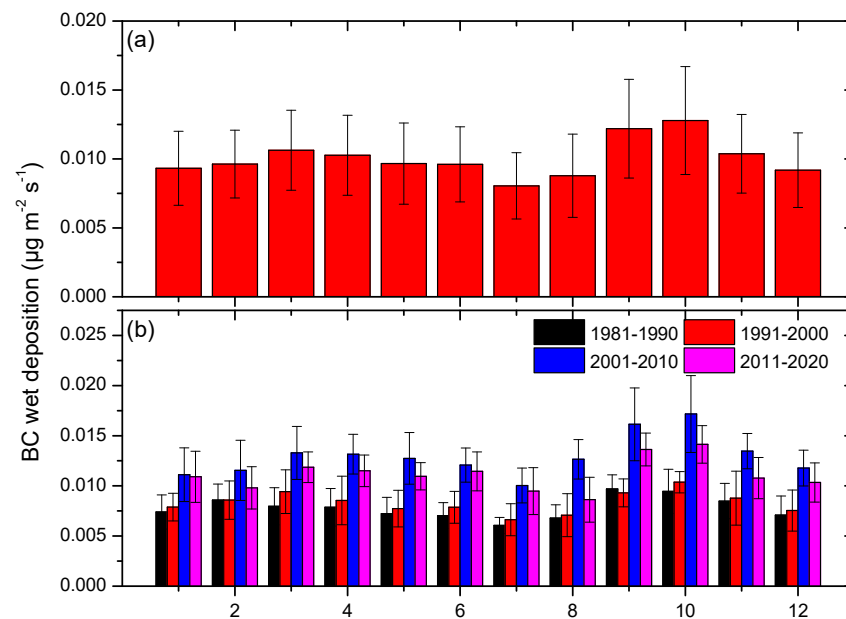


**Figure 7.** Monthly variations of area-averaged black carbon wet deposition flux over the Sichuan basin from 1981 to 2020 (a) and in four periods (b) during 1981–1990, 1991–2000, 2001–2010, and 2011–2020.

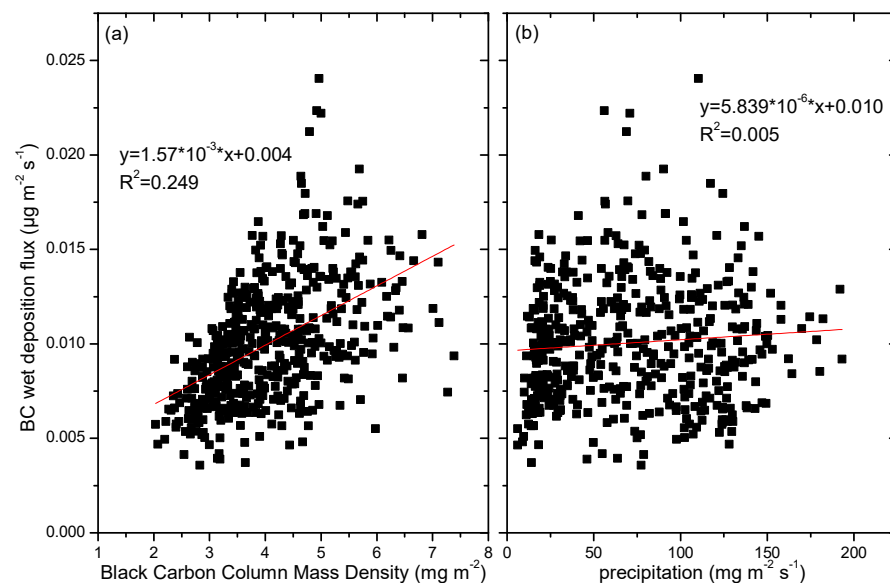


**Figure 8.** Relations between BC wet deposition flux and BC column mass density (a), and precipitation (b).

The spatial distributions of the correlation coefficients of BC wet deposition flux with BC column mass density and precipitation over the Sichuan Basin are shown in Figure 9. As shown in Figure 9b,c, the values of the correlation coefficients reflect the significance of the correlations, and the BC wet deposition flux is highly correlated to BC column mass density or precipitation. However, the significance of the correlation of BC wet deposition flux to the BC column mass density or precipitation is not related to the values of the BC wet deposition flux, which is shown in Figure 9a. That is to say, a high correlation coefficient of BC wet deposition flux with BC column mass density or precipitation is not always relevant to large BC wet deposition flux, indicating complicated nonlinear impacts on BC wet deposition by BC concentration, precipitation, and other potential factors. As illustrated in Figure 9b, a high positive correlation coefficient between BC wet

deposition flux and BC column mass density is seen at all the positions of the Sichuan Basin, and its values are in a range of 0.794–0.931. Small-scale secondary circulation and relatively lower thermal inversion caused by the plateau topography in the western part of the Sichuan Basin can lead to the accumulation of aerosols at 0.8–1.4 km above ground level [65]. The economic prosperity and large population in the northwestern part of the Sichuan Basin (e.g., the city of Chengdu) and many heavy industries in the southwestern region (e.g., the city of Leshan) produce plenty of black carbon. These generated BC may contribute to large BC wet deposition flux in the southwestern and northwestern parts of the Sichuan Basin, and a high correlation coefficient is seen. As shown in Figure 9c, the correlation coefficient of BC wet deposition flux with precipitation is smaller than its correlation coefficient with BC column mass density. For the spatial distribution, high BC wet deposition flux generally corresponds to a positive correlation coefficient of BC wet deposition flux with precipitation. This may indicate that precipitation contributes to high BC wet deposition due to the scavenging of BC particles by precipitation. In the process of precipitation, black carbon particles migrate through Brownian motion, inertial collision, and the effects of heat, turbulence, electric charge, and concentration gradient, and are finally captured by falling water droplets or ice crystals. However, it should be noted that excessive precipitation can inhibit the wet deposition of black carbon [64]. In general, BC column mass density and precipitation are two significant factors affecting the spatial and temporal distribution of BC wet deposition flux, and BC wet deposition flux is more related to BC column mass density than to precipitation over the Sichuan Basin.

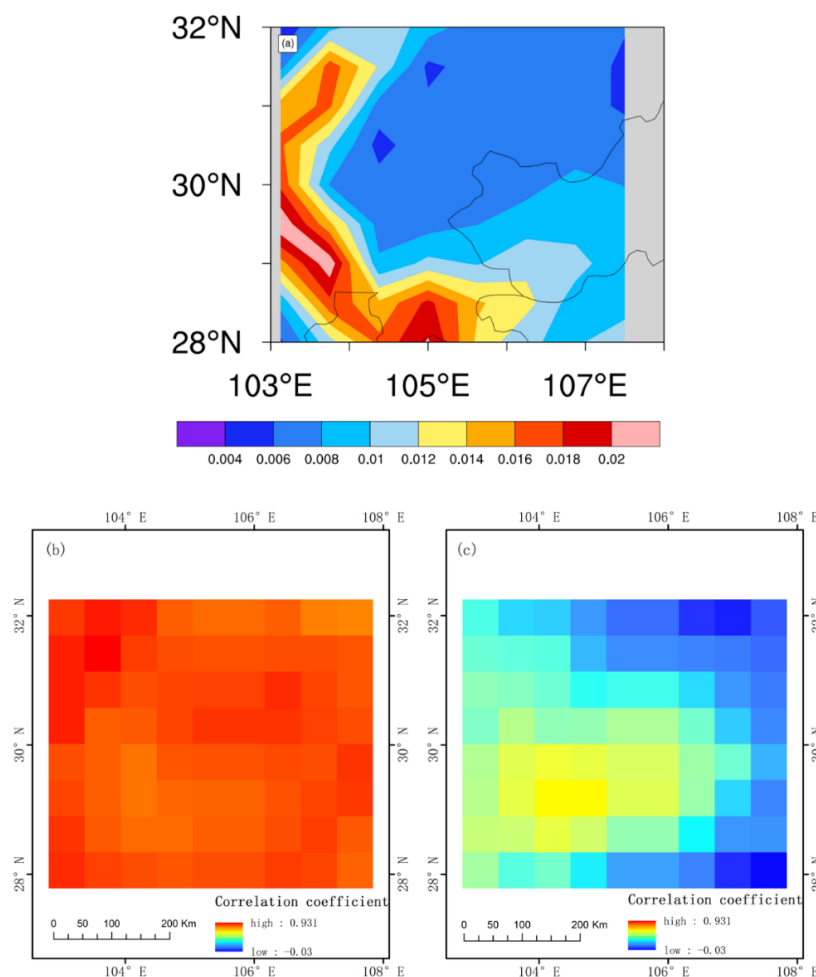


**Figure 9.** The spatial distribution of BC wet deposition flux (unit:  $\mu\text{g m}^{-2} \text{s}^{-1}$ ) (a), and spatial distributions of correlation coefficients of BC wet deposition flux with BC column mass density (b) and precipitation (c) over the Sichuan basin.

To understand the high BC wet deposition flux over the western and southern parts of the Sichuan Basin, two areas with high BC wet deposition fluxes named region A ( $28^{\circ}$  N– $31^{\circ}$  N,  $103^{\circ}$  E– $104^{\circ}$  E) and region B ( $28^{\circ}$  N– $29^{\circ}$  N,  $104^{\circ}$  E– $106^{\circ}$  E) are selected and shown in Figure 1b. A wet deposition-concentration-precipitation (WETD-C-P) diagram is constructed for regions A and B with high BC wet deposition fluxes and is shown in Figure 10. The WETD-C-P diagrams in both regions show complicated features, indicating complex and combined effects of BC column mass density and precipitation on high BC wet deposition flux. As portrayed in Figure 10, larger BC column mass density or precipitation can generally result in higher BC wet deposition flux.

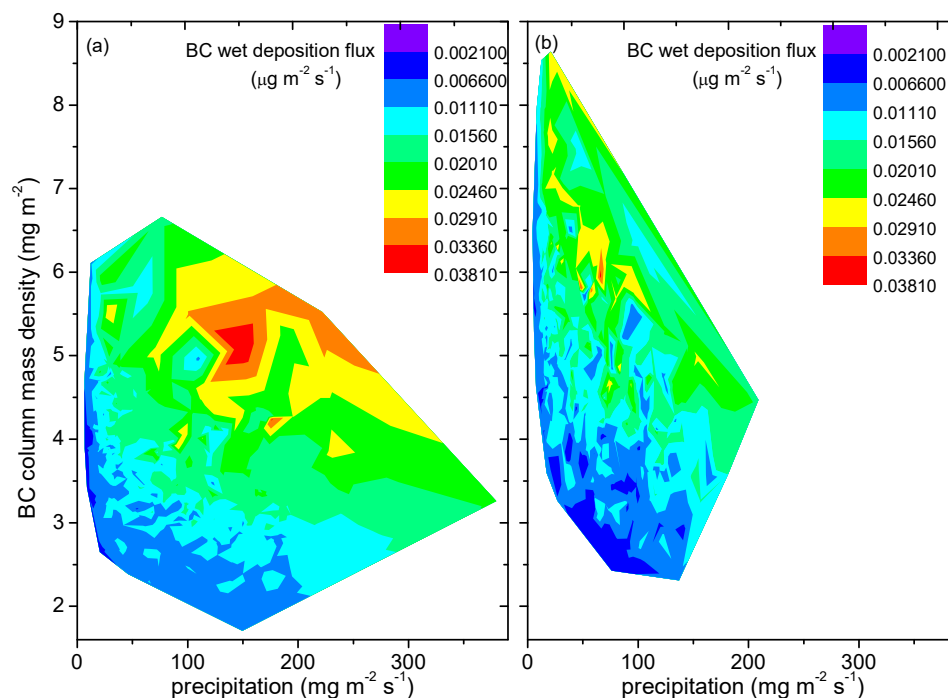


**Figure 10.** The wet deposition-concentration-precipitation (WETD-C-P) relationships. The relationships of monthly BC wet deposition flux with precipitation and BC column mass density in region A ( $28^{\circ}$  N– $31^{\circ}$  N,  $103^{\circ}$  E– $104^{\circ}$  E) (a) and region B ( $28^{\circ}$  N– $29^{\circ}$  N,  $104^{\circ}$  E– $106^{\circ}$  E) (b).

#### 4. Conclusions

In this study, we investigate long-term characteristics of wet deposition flux of black carbon over the Sichuan Basin during 1981–2020 on the basis of the MEERA-2 data. In China, the highest BC wet deposition flux is observed over the Sichuan Basin with an annual-averaged value of  $1.00 \times 10^{-2} \mu\text{g m}^{-2} \text{s}^{-1}$ . The seasonality of BC wet deposition flux depicts maximum mean levels in autumn ( $1.18 \times 10^{-2} \mu\text{g m}^{-2} \text{s}^{-1}$ ), moderate levels in spring ( $1.02 \times 10^{-2} \mu\text{g m}^{-2} \text{s}^{-1}$ ) and winter ( $9.31 \times 10^{-3} \mu\text{g m}^{-2} \text{s}^{-1}$ ), and minimum levels in summer ( $8.81 \times 10^{-3} \mu\text{g m}^{-2} \text{s}^{-1}$ ). The low BC wet deposition flux in summer is mainly due to the small BC concentration, while the low BC wet deposition flux in winter could be attributed to the sparse precipitation amount. The monthly mean BC wet deposition flux varies almost twofold, ranging from the lowest mean value of  $8.05 \times 10^{-3} \mu\text{g m}^{-2} \text{s}^{-1}$  in July to the highest  $1.28 \times 10^{-2} \mu\text{g m}^{-2} \text{s}^{-1}$  in October. BC column mass density and precipitation are two significant factors affecting the spatial and temporal distribution of BC wet deposition flux, and positive correlations of BC wet deposition flux with BC column mass density or precipitation are seen for high BC wet deposition. Nevertheless, BC wet deposition flux is found to be more related to BC column mass density than to precipitation over the Sichuan Basin.

**Author Contributions:** Conceptualization, Y.Z. and X.Z.; Methodology, Y.Z. and X.Z.; Software, Y.Z., X.Z. and Y.W.; Validation, Y.Z. and X.Z.; Formal analysis, Y.Z. and X.Z.; Investigation, Y.Z. and X.Z.; Resources, X.Z.; Data curation, Y.Z. and X.Z.; Writing—original draft, Y.Z.; Writing—review & editing, X.Z.; Visualization, Y.Z.; Project administration, X.Z.; Funding acquisition, X.Z. All authors have read and agreed to the published version of the manuscript.

**Funding:** This paper is sponsored by the Qing Lan Project.

**Institutional Review Board Statement:** Not applicable.

**Informed Consent Statement:** Not applicable.

**Data Availability Statement:** Data are available upon request.

**Acknowledgments:** This paper is supported by the Qinglan Project. We used the data produced with the Giovanni data system and developed and maintained by the NASA GES DISC in this study. We also acknowledge the mission scientists and Principal Investigators who provided the data used in this research effort.

**Conflicts of Interest:** The authors declare no conflict of interest.

## References

1. Bond, T.C.; Doherty, S.J.; Fahey, D.W.; Forster, P.M.; Bernsten, T.; DeAngelo, B.J.; Flanner, M.G.; Ghan, S.; Kärcher, B.; Koch, D.; et al. Bounding the role of black carbon in the climate system: A scientific assessment. *J. Geophys. Res. Atmos.* **2013**, *118*, 5380–5520. [[CrossRef](#)]
2. Wang, Q.Y.; Huang, R.J.; Cao, J.J.; Tie, X.X.; Shen, Z.X.; Zhao, S.Y.; Han, Y.M.; Li, G.H.; Li, Z.Q.; Ni, H.Y.; et al. Contribution of regional transport to the black carbon aerosol during winter haze period in Beijing. *Atmos. Environ.* **2016**, *132*, 11–18. [[CrossRef](#)]
3. Homann, K.H. Fullerenes and soot formation—new pathways to large particles in flames. *Angew. Chem. Int. Ed.* **1998**, *37*, 2434–2451. [[CrossRef](#)]
4. Custodio, D.; Cerqueira, M.; Fialho, P.; Nunes, T.; Pio, C.; Henriques, D. Wet deposition of particulate carbon to the central North Atlantic Ocean. *Sci. Total Environ.* **2014**, *496*, 92–99. [[CrossRef](#)]
5. Zhang, Y.L.; Cerqueira, M.; Salazar, G.; Zotter, P.; Hueglin, C.; Zellweger, C.; Pio, C.; Prevot, A.S.H.; Szidat, S. Wet deposition of fossil and non-fossil derived particulate carbon: Insights from radiocarbon measurement. *Atmos. Environ.* **2015**, *115*, 257–262. [[CrossRef](#)]
6. Iavorivska, L.; Boyer, E.W.; DeWalle, D.R. Atmospheric deposition of organic carbon via precipitation. *Atmos. Environ.* **2016**, *146*, 153–163. [[CrossRef](#)]
7. Sorokina, V.V.; Soier, V.G. Dry and wet atmospheric deposition of organic carbon in coastal and water areas of the northeastern part of the Sea of Azov. *Oceanology* **2016**, *56*, 733–741. [[CrossRef](#)]
8. Wang, Q.; Feng, W.; Liu, M.; Xu, H. Atmospheric elemental carbon deposition from urban and suburban sites of Shanghai: Characteristics, sources and comparison with aerosols and soils. *Atmos. Pollut. Res.* **2021**, *12*, 193–199. [[CrossRef](#)]
9. Warneck, P. *Chemistry of the Natural Atmosphere*, 2nd ed.; Academic Press: New York, NY, USA, 1999; p. 444.
10. Cerqueira, M.; Pio, C.; Legrand, M.; Puxbaum, H.; Kasper-Giebl, A.; Afonso, J.; Preunkert, S.; Gelencsér, A.; Fialho, P. Particulate carbon in precipitation at European background sites. *Aerosol Sci.* **2010**, *41*, 51–61. [[CrossRef](#)]
11. Kardel, F.; Wuyts, K.; Maher, B.A.; Samson, R. Intra-urban spatial variation of magnetic particles: Monitoring via leaf saturation isothermal remanent magnetization (SIRM). *Atmos. Environ.* **2012**, *55*, 111–120. [[CrossRef](#)]
12. Yang, F.; Mitra, P.; Zhang, L.; Prak, L.; Verherbruggen, Y.; Kim, J.S.; Sun, L.; Zheng, K.; Tang, K.; Auer, M. Engineering secondary cell wall deposition in plants. *Plant Biotechnol. J.* **2012**, *11*, 325–335. [[CrossRef](#)] [[PubMed](#)]
13. Pan, Y.P.; Wang, Y.S. Atmospheric wet and dry deposition of trace elements at 10 sites in Northern China. *Atmos. Chem. Phys.* **2015**, *15*, 951–972. [[CrossRef](#)]
14. Nho-Kim, E.; Michou, M.; Peuch, V. Parameterization of size-dependent particle dry deposition velocities for global modeling. *Atmos. Environ.* **2004**, *38*, 1933–1942. [[CrossRef](#)]
15. Quérel, A.; Monier, M.; Flossmann, A.I.; Lemaitrea, P.; Porcherona, E. The importance of new collection efficiency values including the effect of rear capture for the below cloud scavenging of aerosol particles. *Atmos. Res.* **2014**, *142*, 57–66. [[CrossRef](#)]
16. Sic, B.; Amraoui, L.E.; Marécal, V.; Josse, B.; Arteta, J.; Guth, J.; Joly, M.; Hamer, P.D. Modelling of primary aerosols in the chemical transport model MOCAGE: Development and evaluation of aerosol physical parameterizations. *Geosci. Model Dev.* **2015**, *8*, 381–408. [[CrossRef](#)]
17. Zhu, J.X.; He, N.P.; Wang, Q.F.; Yuan, G.F.; Wen, D.; Yu, G.R.; Jia, Y.L. The composition, spatial patterns, and influencing factors of atmospheric wet nitrogen deposition in Chinese terrestrial ecosystems. *Sci. Total Environ.* **2015**, *511*, 777–785. [[CrossRef](#)]
18. Luo, X.S.; Pan, Y.P.; Goulding, K.; Zhang, L.; Liu, X.J.; Zhang, F.S. Spatial and seasonal variations of atmospheric sulfur concentrations and dry deposition at 16 rural and suburban sites in China. *Atmos. Environ.* **2016**, *146*, 79–89. [[CrossRef](#)]
19. Xu, W.; Zhao, Y.H.; Liu, X.J.; Dore, A.J.; Zhang, L.; Liu, L.; Cheng, M.M. Atmospheric nitrogen deposition in the Yangtze River basin: Spatial pattern and source attribution. *Environ. Pollut.* **2018**, *232*, 546–555. [[CrossRef](#)]

20. Yan, F.; Wang, P.; Kang, S.; Chen, P.; Li, C. High particulate carbon deposition in Lhasa—a typical city in the Himalayan–Tibetan Plateau due to local contributions. *Chemosphere* **2020**, *247*, 125843. [[CrossRef](#)]
21. Niu, Z.; Huang, Z.; Wang, S.; Feng, X.; Wu, S.; Zhao, H.; Lu, X. Characteristics and source apportionment of particulate carbon in precipitation based on dual-carbon isotopes ( $^{13}\text{C}$  and  $^{14}\text{C}$ ) in Xian, China. *Environ. Pollut.* **2022**, *299*, 118908. [[CrossRef](#)]
22. Hegg, D.A.; Clarke, A.D.; Doherty, S.J.; Ström, J. Measurements of black carbon aerosol washout ratio on Svalbard. *Tellus B Chem. Phys. Meteorol.* **2011**, *63*, 891–900. [[CrossRef](#)]
23. Mori, T.; Kondo, Y.; Ohata, S.; Moteki, N.; Matsui, H.; Oshima, N.; Iwasaki, A. Wet deposition of black carbon at a remote site in the East China Sea. *J. Geophys. Res. Atmos.* **2014**, *119*, 10485–10498. [[CrossRef](#)]
24. Wang, Z.W.; Gallet, J.C.; Pedersen, C.A.; Zhang, X.S.; Ström, J.; Ci, Z.J. Elemental carbon in snow at Changbai Mountain, northeastern China: Concentrations, scavenging ratios, and dry deposition velocities. *Atmos. Chem. Phys.* **2014**, *14*, 14221–14248. [[CrossRef](#)]
25. Hadley, O.L.; Corrigan, C.; Ramanathan, V. *Measurements of Black Carbon in California Snow and Rain*; California Energy Commission, PIER Energy-Related Environmental Research Program: Sacramento, CA, USA, 2007.
26. Ohata, S.; Moteki, N.; Kondo, Y. Evaluation of a Method for measurement of the concentration and size distribution of black carbon particles suspended in rainwater. *Aerosol Sci. Technol.* **2011**, *45*, 1326–1336. [[CrossRef](#)]
27. Willey, J.D.; Kieber, R.J.; Eyman, M.S.; Avery, G.B. Rainwater Dissolved Organic Carbon: Concentrations and Global Flux. *Glob. Biogeochem. Cycles* **2000**, *14*, 139–148. [[CrossRef](#)]
28. Wu, M.X.; Liu, X.H.; Zhang, L.M.; Wu, C.L.; Lu, Z.; Ma, P.L.; Wang, H.L.; Tilmes, S.; Mahowald, N.; Matsui, H.; et al. Impacts of aerosol dry deposition on black carbon spatial distributions and radiative effects in the Community Atmosphere Model CAM5. *J. Adv. Model. Earth Syst.* **2018**, *10*, 1150–1171. [[CrossRef](#)]
29. Matsumoto, K.; Kodama, S.; Sakata, K.; Watanabe, Y. Atmospheric deposition fluxes and processes of the water-soluble and water-insoluble organic carbon in central Japan. *Atmos. Environ.* **2022**, *271*, 118913. [[CrossRef](#)]
30. Coelho, C.H.; Francisco, J.G.; Nogueira, R.F.P.; Campos, M.L.A.M. Dissolved Organic Carbon in Rainwater from Areas Heavily Impacted by Sugar Cane Burning. *Atmos. Environ.* **2008**, *30*, 7115–7121. [[CrossRef](#)]
31. Zeng, J.; Yu, F.J.; Xia, M.; Wan, Z.J.; Wu, Q.X.; Qin, C.Q. Dissolved organic carbon in rainwater from a karst agricultural area of Southwest China: Variations, sources, and wet deposition fluxes. *Atmos. Res.* **2020**, *245*, 105140. [[CrossRef](#)]
32. Niu, H.; Kang, S.C.; Shi, X.F.; Zhang, G.T.; Wang, S.J.; Pu, T. Dissolved organic carbon in summer precipitation and its wet deposition flux in the Mt. Yulong region, southeastern Tibetan Plateau. *J. Atmos. Chem.* **2019**, *76*, 1–20. [[CrossRef](#)]
33. Zhao, H.H.; Chen, L.Q.; Yan, J.P.; Shi, P.; Li, Y.; Li, W. Characteristics of Particulate Carbon in Precipitation during the Rainy Season in Xiamen Island, China. *Atmosphere* **2016**, *7*, 140. [[CrossRef](#)]
34. Pan, Y.P.; Wang, Y.S.; Xin, J.Y.; Tang, G.Q.; Song, T.; Wang, Y.H.; Li, X.R.; Wu, F.K. Study on Dissolved Organic Carbon in Precipitation in Northern China. *Atmos. Environ.* **2010**, *44*, 2350–2357. [[CrossRef](#)]
35. Orlović-Leko, P.; Plavšić, M.; Bura-Nakić, E.; Kozarac, Z.; Čosović, B. Organic Matter in the Bulk Precipitations in Zagreb and Šibenik, Croatia. *Atmos. Environ.* **2009**, *43*, 805–811. [[CrossRef](#)]
36. Kanakidou, M.; Duce, R.A.; Prospero, J.M.; Baker, A.R.; Benitez-Nelson, C.; Dentener, F.J.; Hunter, K.A.; Liss, P.S.; Mahowald, N.; Okin, G.S. Atmospheric Fluxes of Organic N and P to the Global Ocean. *Glob. Biogeochem. Cycles* **2012**, *26*, 1–12. [[CrossRef](#)]
37. Matsuda, K.; Sase, H.; Murao, N.; Fukazawa, T.; Khoomsab, K.; Chanonmuang, P.; Visaratana, T.; Khummongkol, P. Dry and wet deposition of elemental carbon on a tropical forest in Thailand. *Atmos. Environ.* **2012**, *54*, 282–287. [[CrossRef](#)]
38. Jacobi, H.W.; Obleitner, F.; Da Costa, S.; Ginot, P.; Eleftheriadis, K.; Aas, W.; Zannata, M. Deposition of ionic species and black carbon to the Arctic snowpack: Combining snow pit observations with modeling. *Atmos. Chem. Phys.* **2019**, *19*, 10361–10377. [[CrossRef](#)]
39. Zhu, S.B.; Xiao, Z.S.; Che, H.Z.; Chen, Q.L. Impact of aerosols on warm clouds over the Sichuan Basin, China in winter based on the MERRA-2 reanalysis dataset. *Atmos. Pollut. Res.* **2022**, *13*, 101342. [[CrossRef](#)]
40. Zhao, S.P.; Yu, Y.; Yin, D.Y.; Qin, D.H.; He, J.J.; Dong, L.X. Spatial patterns and temporal variations of six criteria air pollutants during 2015 to 2017 in the city clusters of Sichuan Basin, China. *Sci. Total Environ.* **2018**, *624*, 540–557. [[CrossRef](#)]
41. Randles, C.A.; da Silva, A.M.; Buchard, V.; Colarco, P.R.; Darmenov, A.; Govindaraju, R.; Smirnov, A.; Holben, B.; Ferrare, R.; Hair, J.; et al. The MERRA-2 aerosol reanalysis, 1980 onward. Part I: System description and data assimilation evaluation. *J. Clim.* **2017**, *30*, 6823–6850. [[CrossRef](#)]
42. Buchard, V.; Randles, C.A.; da Silva, A.M.; Darmenov, A.; Colarco, P.R.; Govindaraju, R.; Ferrare, R.; Hair, J.; Beyersdorf, A.J.; Ziemba, L.D.; et al. The MERRA-2 aerosol reanalysis, 1980 onward. Part II: Evaluation and case studies. *J. Clim.* **2017**, *30*, 6851–6872. [[CrossRef](#)]
43. Gelaro, R.; McCarty, W.; Suárez, M.J.; Todling, R.; Molod, A.; Takacs, L.; Randles, C.A.; Darmenov, A.; Bosilovich, M.G.; Reichle, R.; et al. The Modern-Era retrospective analysis for research and applications, version 2 (MERRA-2). *J. Clim.* **2017**, *30*, 5419–5454. [[CrossRef](#)] [[PubMed](#)]
44. Hung, W.T.; Lu, C.; Wang, S.H.; Chen, S.P.; Tsai, F.; Chou, C.K. Investigation of long-range transported PM<sub>2.5</sub> events over Northern Taiwan during 2005–2015 winter seasons. *Atmos. Environ.* **2019**, *217*, 116920. [[CrossRef](#)]
45. Global Modeling and Assimilation Office. Available online: <https://gmao.gsfc.nasa.gov/reanalysis/MERRA-2/> (accessed on 3 July 2019).

46. Chen, Y.T.; Gao, Y.; Wu, S.L.; Zhang, L.; Wang, Q.Q.; Yao, X.H.; Gao, H.W. Wet deposition of atmospheric selenium and sensitivity to emission and precipitation patterns. *Sci. Total Environ.* **2022**, *835*, 155402. [[CrossRef](#)]
47. Huo, M.Q.; Sato, K.; Ohizumi, T.; Akimoto, H.; Takahashi, K. Characteristics of carbonaceous components in precipitation and atmospheric particle at Japanese sites. *Atmos. Environ.* **2016**, *146*, 164–173. [[CrossRef](#)]
48. Zhang, X.Y.; Zhao, L.M.; Cheng, M.M.; Liu, H.L.; Wang, Z.; Wu, X.D.; Yu, H. Long-term changes in wet nitrogen and sulfur deposition in Nanjing. *Atmos. Environ.* **2018**, *195*, 104–111. [[CrossRef](#)]
49. Cao, S.S.; Zhang, S.Q.; Gao, C.C.; Yan, Y.Y.; Bao, J.H.; Su, L.; Liu, M.Q.; Peng, N.N.; Liu, M. A long-term analysis of atmospheric black carbon MERRA-2 concentration over China during 1980–2019. *Atmos. Environ.* **2021**, *264*, 118662. [[CrossRef](#)]
50. Yuan, X.; Zuo, J. Transition to low carbon energy policies in China—From the Five-Year Plan perspective. *Energy Policy* **2011**, *39*, 3855–3859. [[CrossRef](#)]
51. Xu, X.F.; Yang, X.Y.; Zhu, B.; Tang, Z.W.; Wu, H.; Xie, L.F. Characteristics of MERRA-2 black carbon variation in east China during 2000–2016. *Atmos. Environ.* **2020**, *222*, 117140. [[CrossRef](#)]
52. Wang, H.; Tian, M.; Chen, Y.; Shi, G.; Liu, Y.; Yang, F.; Zhang, L.; Deng, L.; Yu, J.; Peng, C.; et al. Seasonal characteristics, formation mechanisms and source origins of PM<sub>2.5</sub> in two megacities in Sichuan Basin, China. *Atmos. Chem. Phys.* **2018**, *18*, 865–881. [[CrossRef](#)]
53. Feng, X.; Wei, S.; Wang, S. Temperature inversions in the atmospheric boundary layer and lower troposphere over the Sichuan Basin, China: Climatology and impacts on air pollution. *Sci. Total Environ.* **2020**, *726*, 138579. [[CrossRef](#)]
54. Yu, G.; Jia, Y.; He, N.; Zhu, J.; Chen, Z.; Wang, Q.; Piao, S.; Liu, X.; He, H.; Guo, X. Stabilization of atmospheric nitrogen deposition in China over the past decade. *Nat. Geosci.* **2019**, *12*, 424–429. [[CrossRef](#)]
55. Yan, F.P.; He, C.L.; Kang, S.C.; Chen, P.F.; Hu, Z.F.; Han, X.W.; Gautam, S.; Yan, C.Q.; Zheng, M.; Sillanpaa, M.; et al. Deposition of Organic and Black Carbon: Direct Measurements at Three Remote Stations in the Himalayas and Tibetan Plateau. *J. Geophys. Res. Atmos.* **2019**, *124*, 9702–9715. [[CrossRef](#)]
56. Zhou, W.B.; Xiang, W.H.; You, Y.Y.; Ouyang, S.; Zhao, Z.H.; Zhang, S.L.; Zeng, Y.L.; Li, J.R.; Wang, J.R.; Wang, K.L. Atmospheric Wet Deposition of Organic Carbon and Dissolved Nitrogen in City, Countryside and Nature Reserve of Subtropical China. *J. Am. Water Resour. Assoc.* **2020**, *56*, 1045–1058. [[CrossRef](#)]
57. Zhang, X.; Huang, Y.; Rao, R. Aerosol characteristics including fumigation effect under weak precipitation over the southeastern coast of China. *J. Atmos. Sol.-Terr. Phys.* **2012**, *84–85*, 25–36. [[CrossRef](#)]
58. Yang, F.; He, K.; Ye, B.; Chen, X.; Cha, S.H.; Cadle, S.H.; Chan, T.; Mulawa, P.A. One-year record of organic and elemental carbon in fine particles in downtown Beijing and Shanghai. *Atmos. Chem. Phys.* **2005**, *5*, 1449–1457. [[CrossRef](#)]
59. Witkowska, A.; Lewandowska, A.; Falkowska, L.M. Parallel measurements of organic and elemental carbon dry (PM<sub>1</sub>, PM<sub>2.5</sub>) and wet (rain, snow, mixed) deposition into the Baltic Sea. *Mar. Pollut. Bull.* **2016**, *104*, 303–312. [[CrossRef](#)] [[PubMed](#)]
60. Zhang, Q.Y.; Wang, Q.F.; Zhu, J.X.; Xu, L.; Chen, Z.; Xiao, J.F.; He, N.P. Spatiotemporal variability, source apportionment, and acid-neutralizing capacity of atmospheric wet base-cation deposition in China. *Environ. Pollut.* **2020**, *262*, 114335. [[CrossRef](#)] [[PubMed](#)]
61. Yu, X.; Pan, Y.P.; Song, W.; Li, S.; Li, D.; Zhu, M.; Zhou, H.S.; Zhang, Y.L.; Li, D.J.; Yu, J.Z.; et al. Wet and Dry Nitrogen Depositions in the Pearl River Delta, South China: Observations at Three Typical Sites With an Emphasis on Water-Soluble Organic Nitrogen. *J. Geophys. Res. Atmos.* **2020**, *125*, e2019JD030983. [[CrossRef](#)]
62. Chen, Z.L.; Huang, T.; Huang, X.H.; Han, X.X.; Yang, H.; Cai, Z.C.; Yao, L.; Han, X.; Zhang, M.G.; Huang, C.C. Characteristics, sources and environmental implications of atmospheric wet nitrogen and sulfur deposition in Yangtze River Delta. *Atmos. Environ.* **2019**, *219*, 116904. [[CrossRef](#)]
63. Zhao, H.B.; Zheng, C.G. Monte Carlo solution of wet removal of aerosols by precipitation. *Atmos Environ.* **2006**, *40*, 1510–1525. [[CrossRef](#)]
64. Wu, Y.N.; Liu, J.K.; Zhai, J.X.; Cong, L.; Wang, Y.; Ma, W.M.; Zhang, Z.M.; Li, C.Y. Comparison of dry and wet deposition of particulate matter in near-surface waters during summer. *PLoS ONE* **2018**, *13*, e0199241. [[CrossRef](#)] [[PubMed](#)]
65. Yuan, L.; Zhang, X.L.; Che, Y.Z.; Xia, X.A.; Liu, X.; Zhao, T.L.; Song, M.H. Vertical profile and radiative forcing of black carbon in a winter pollution period over Chengdu, China. *Atmos. Res.* **2022**, *265*, 105896. [[CrossRef](#)]

**Disclaimer/Publisher’s Note:** The statements, opinions and data contained in all publications are solely those of the individual author(s) and contributor(s) and not of MDPI and/or the editor(s). MDPI and/or the editor(s) disclaim responsibility for any injury to people or property resulting from any ideas, methods, instructions or products referred to in the content.